NASA TECHNICAL NOTE

NASA TN D-3449

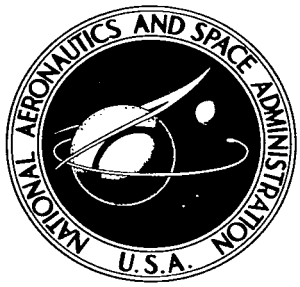

NASA TN D-3449

EFFECTS OF SUBCOOLING AND GRAVITY LEVEL ON BOILING IN THE DISCRETE BUBBLE REGION

by Thomas H. Cochran and John C. Aydelott

Lewis Research Center
Cleveland, Ohio

NATIONAL AERONAUTICS AND SPACE ADMINISTRATION • WASHINGTON, D. C. • SEPTEMBER 1966

NASA TN D-3449

EFFECTS OF SUBCOOLING AND GRAVITY LEVEL ON BOILING IN THE DISCRETE BUBBLE REGION

By Thomas H. Cochran and John C. Aydelott

Lewis Research Center
Cleveland, Ohio

NATIONAL AERONAUTICS AND SPACE ADMINISTRATION

For sale by the Clearinghouse for Federal Scientific and Technical Information
Springfield, Virginia 22151 – Price $2.00

EFFECTS OF SUBCOOLING AND GRAVITY LEVEL ON BOILING IN THE DISCRETE BUBBLE REGION

by Thomas H. Cochran and John C. Aydelott

Lewis Research Center

SUMMARY

The effects of changes in subcooling and gravity level are investigated for water boiling at low heat flux from a flat horizontal surface. The zero gravity data were obtained by allowing the experimental package to free fall in a 100-foot drop tower, which permitted the attainment of less than 10^{-5} times Earth gravity. An analysis of the dynamics of a generated bubble resulted in a new approach to the formulation of the buoyancy force and the definition of a force associated with the unbalanced pressure across the top surface of the bubble. The force associated with liquid inertia was obtained by the use of Newton's second law of motion. Application of the analysis to experimental data indicated that this newly defined pressure force was of major importance in bringing about bubble separation. Additional investigation showed that nucleate boiling was independent of gravity at high subcooling.

INTRODUCTION

The coming of space exploration has prompted investigations of the effect of gravity level on the transfer of heat to fluids. A particular area of interest has been the storage of cryogenic fluids in closed containers over long periods of time, as would occur on a coasting space flight. Under such conditions, the fluid may be subject to zero gravity subcooled nucleate boiling because of a relatively low heat flux from solar radiation.

In recent years, a great deal of experimental work with nucleate boiling of saturated fluids in various gravity fields has been conducted (refs. 1 to 17). These investigations have shown that, in the low heat flux region, the boiling mechanism is dependent on the dynamics of vapor bubbles formed on the heated surface. Experimental studies of the effect of subcooling on nucleate boiling in normal gravity by the University of Denver (refs. 18 to 20) also indicate this dependence. Analytical works, such as references 21

to 24, propose the importance of bubble dynamics.

The present work is concerned with the effect of subcooling and gravity level on the dynamics of steam bubbles formed on a flat horizontal surface. High-speed motion pictures were taken at subcoolings of approximately 5^{o}, 10^{o}, 15^{o}, 25^{o}, 35^{o}, and 40^{o} F in normal gravity and in an environment of less than 10^{-5} times normal gravity. The heat flux selected was kept constant for all tests and set at a level in the range defined in normal gravity as the discrete bubble region (ref. 13). In such a range in normal gravity, the bubbles generally grow undisturbed on the heated surface, and the heat-transfer mechanism is highly dependent on the disturbance in the liquid caused by the growth and departure of the bubbles.

Analysis of the photographic data included measurements of growth characteristics of the bubbles and calculation of the forces acting on the bubbles during their growth. The formulation for the forces included a new treatment of the buoyancy force and the definition of a force concerned with the unbalanced pressure across the top surface of the bubble. An original approach to the force associated with liquid inertia resulted from the use of Newton's second law of motion. From force histories, interpretations regarding the dynamic effects are made and discussed.

Motion picture supplement C-246, which shows the experimental procedure and subcooled boiling of water at the various test conditions, has been prepared and is available on loan. A request card and a description of the film are included at the back of this report.

SYMBOLS

A	area, ft^2
C_{Dr}	drag coefficient
d	diameter, ft
F_B	buoyancy force, lb force
F_{Dr}	drag force, lb force
F_{Dy}	dynamic force, lb force
F_P	pressure force, lb force
F_R	total removal force, lb force
F_S	total surface tension force, lb force
F_{S_y}	vertical component of surface tension force, lb force
g	acceleration due to gravity, ft/sec^2

g_c gravitational constant, (lb mass/lb force)(ft/sec^2)

g_0 standard acceleration of gravity on Earth, ft/sec^2

M mass, lb mass

P pressure, lb force/sq ft

R radius, ft

r general radius, ft

T radius of curvature of top surface, ft

t time, sec

V bubble total volume, ft^3

V_b bubble volume directly over base, ft^3

Y bubble center of mass, ft

y distance above heater surface, ft

ν velocity, ft/sec

ρ density, lb mass/ft^3

μ dynamic viscosity, (lb force)(sec)/ft^2

σ surface tension, lb force/ft

φ contact angle

Subscripts:

b base

i inside bubble

ℓ liquid

max maximum

o outside bubble

S heater surface

sat saturated vapor

v vapor

1 location one

2 location two

ANALYSIS

Bubble Model

In order to calculate the volume and center of mass of the generated vapor masses, a bubble model is assumed. The only restrictions placed on the model are that it is symmetric with respect to the y-axis, as shown in figure 1, and that the surface of the bubble directly over the base is spherical. The general nature of this model is prompted by Warner (ref. 18), who shows that, for subcooled conditions, specification of a particular bubble geometry, such as a sphere, is in error.

Simple geometric formulas cannot be used to calculate bubble total volume because of the general nature of the model. Consequently, volume is determined by an integrative method in which a bubble is divided into segments, the volumes of which can be approximated if they are assumed to be circular disks. The sums of the volumes of the disks produce the total volume. The volume directly over the bubble base is obtained by assuming that the volume is a right circular cylinder with a segment of a sphere as a cap.

The center of mass of a bubble is selected as the characteristic dimension to describe its motion and is determined from the location of the plane parallel to the heater surface, which divides the bubble in half with respect to its total volume.

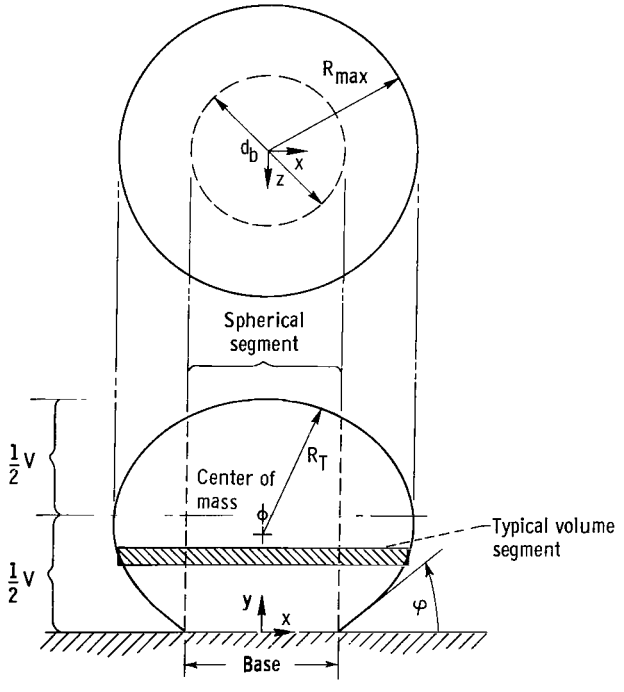

Figure 1. - Bubble model.

Bubble Forces

An analytical investigation of the dynamics of a steam bubble on a heated surface results in the identification of buoyancy, surface tension, pressure, drag, and dynamic forces. The force associated with the vapor weight is neglected because the experimental conditions are such that it is very small. However, for all fluids near the critical thermodynamic state and for some fluids that do not have a large difference between liquid and vapor density, such as hydrogen, this force is large enough to be included.

Buoyancy Force

Buoyancy on an object submerged in a liquid is caused by the difference between the external hydrostatic pressure force on its top surface and the external hydrostatic pressure force on its bottom surface. Therefore, for a bubble attached to a heated surface, the volume of the bubble directly over the base does not generate a buoyant force because of the lack of liquid beneath the base. The buoyancy force, as derived in appendix A, is defined as

$$F_B = (V - V_b)\rho_\ell \frac{g}{g_c} \tag{1}$$

and it acts in a direction opposite to the acceleration due to gravity.

Surface Tension Force

A surface tension force is generated at the boundary of a liquid and some other substance, such as a vapor or a solid. Therefore, such a force exists at the base of a bubble attached to the heater surface at the boundary of the liquid, vapor, and solid surface. The direction of this force is perpendicular to the boundary and in the plane of the liquid-vapor interface. Surface tension is defined as the ratio of the surface force to the length along which the force acts, which, for an attached bubble, is

$$\sigma_S = \frac{F_S}{\pi d_b} \tag{2}$$

The horizontal component of the force is cancelled out around the circumference of the bubble base and only the vertical component remains, such that

$$F_{S_y} = \sigma_S \pi d_b \sin \varphi \tag{3}$$

where the contact angle φ is the angle at the base between the liquid-vapor interface and the heater surface, as shown in figure 1. This force retards the movement of a bubble from the surface.

Pressure Force

The net force due to the uniform internal pressure on a bubble surface is zero for

a bubble surrounded by liquid. For a bubble attached to a surface, however, the net internal pressure force on the spherical surface area directly over the base is unbalanced. Since the pressure is greater inside the bubble than outside, the force acts to remove the bubble from the surface. The detailed derivation of this force in appendix B yields

$$F_P = \frac{1}{2}\left(\frac{\pi d_b^{\,2}}{T}\right)\sigma_{sat} \tag{4}$$

Drag Force

The movement of a mass through a fluid creates a retardation force, which is termed drag. Only an approximation can be made for this force because of a lack of knowledge regarding the motion of the fluid about the bubble. Siegel and Keshock (ref. 4) derived an equation in terms of the drag coefficient in the form

$$F_{Dr} = \frac{1}{2}\rho_\ell C_{Dr}\pi R_{max}^2\left(\frac{dY}{dt}\right)^2 \tag{5}$$

where C_{Dr} was evaluated as

$$C_{Dr} = \frac{45\mu_\ell}{2R_{max}\rho_\ell\left(\frac{dY}{dt}\right)} \tag{6}$$

The University of Denver (ref. 20) used the same equation but evaluated the drag coefficient as

$$C_{Dr} = \frac{48\mu_\ell}{2R_{max}\rho_\ell\left(\frac{dY}{dt}\right)} \tag{7}$$

The larger of the two (eq. (7)) is used in this work, and the result is

$$F_{Dr} = 12\mu_\ell\pi R_{max}\left(\frac{dY}{dt}\right) \tag{8}$$

As shown in the section Effect of Subcooling in Normal Gravity, the selection of the drag coefficient is unimportant in that the force was always very small.

Dynamic Force

The last force to be considered is termed the dynamic force F_{D_y}. This force is associated with effects on the bubble caused by the dynamics of the bubble and the liquid flow field surrounding the bubble. The nature of this dynamic force has not been clearly defined so that direct formulation is speculative. Therefore, in this work, the force is obtained by applying Newton's second law of motion to the generated vapor masses, or

$$\sum F = \frac{d}{dt}(M_v \nu) \tag{9}$$

If it is assumed that the positive force direction is that of increasing y, as shown in figure 1 (p. 4), the left side of equation (9) may be expanded in terms of the identified forces:

$$F_B + F_P - F_{S_y} - F_{Dr} + F_{Dy} = \frac{d}{dt}(M_v \nu) \tag{10}$$

If, at any instant, a bubble is considered to be a rigid body whose motion is described by the movement of its center of mass, the momentum side of the equation may be expanded in terms of measurable quantities such that

$$F_B + F_P - F_{S_y} - F_{Dr} + F_{Dy} = \frac{\rho_v}{g_c}\left(\frac{dV}{dt}\frac{dY}{dt} + V\frac{d^2Y}{dt^2}\right) + \frac{V}{g_c}\frac{dY}{dt}\frac{d\rho_v}{dt} \tag{11}$$

When the bubble is observable on the surface, the absolute pressure changes within the bubble are small, so that the change of vapor density with time may be considered negligible. Therefore, when the last term on the right in equation (11) is dropped and the equation is solved for the dynamic force,

$$F_{Dy} = \frac{\rho_v}{g_c}\left(\frac{dV}{dt}\frac{dY}{dt} + V\frac{d^2Y}{dt^2}\right) + F_{Dr} + F_{S_y} - F_B - F_P \tag{12}$$

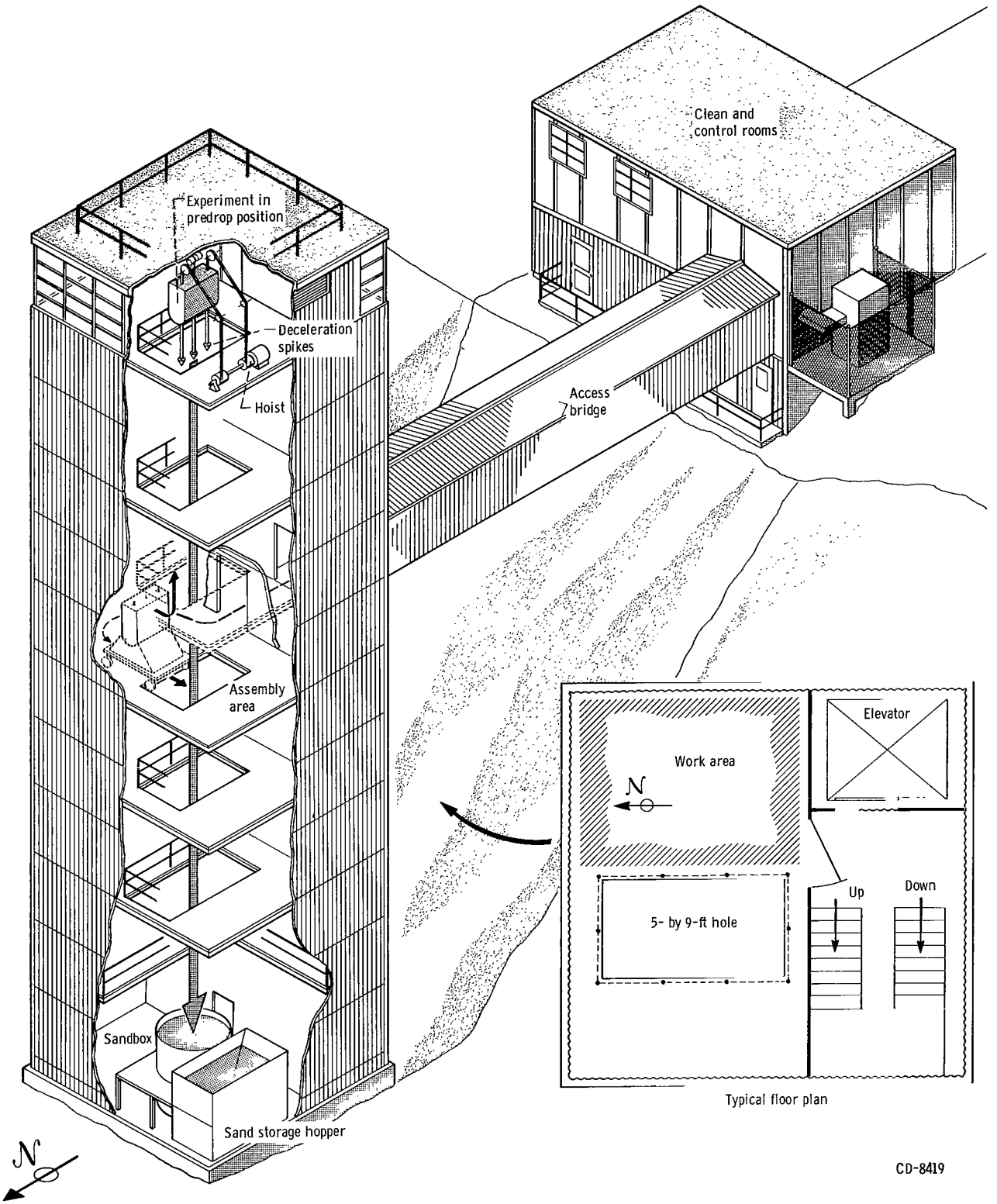

Figure 2. - 100-Foot drop tower.

APPARATUS

100-Foot Drop Tower

The zero gravity experiment results were obtained in the 100-foot drop tower shown in figure 2. A free-fall time of 2.3 seconds was obtained by allowing the experiment package to undergo an 85-foot unguided free fall. The experiment was prepared on the fifth floor of the tower, hoisted to the eighth floor, and suspended from the ceiling by a highly stressed music wire. Release of the experiment was accomplished by pressurization of an air cylinder that forced a knife edge into the support wire, which rested against an anvil. The experimental package was decelerated by allowing wooden spikes 6 feet long, which were mounted on the package, to embed in a box of sand 7 feet deep and 7 feet in diameter.

Drag Shield

Air resistance on the experiment package was reduced by allowing the experiment

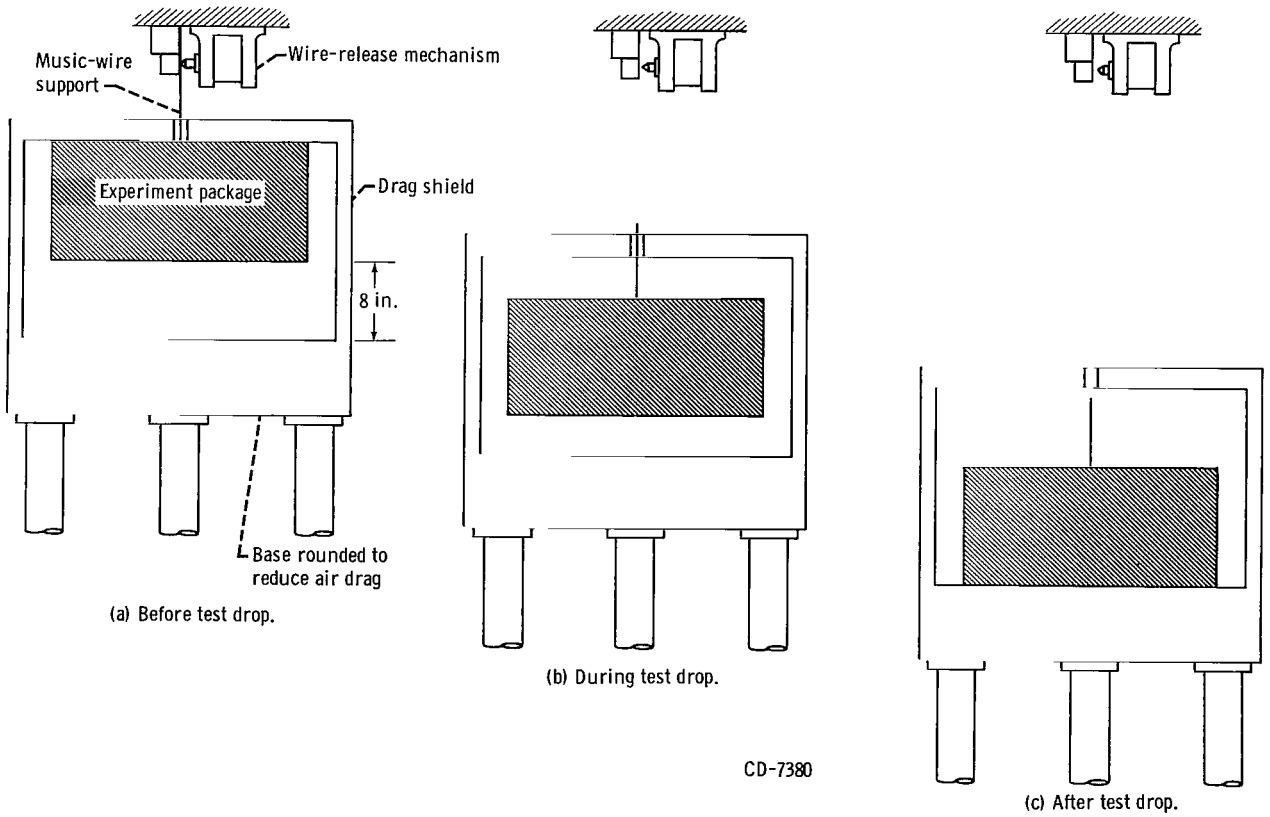

Figure 3. - Schematic drawing showing position of experiment package and drag shield before, during, and after test drop.

to free fall inside a protective air-drag shield as shown in figure 3 (p. 9). The drag shield was designed with a high ratio of weight to frontal area and a low drag coefficient, so that the deviation from true free fall would be minimized. As a result, the experimental package was subjected to a gravity level of less than 10^{-5} g_0. This gravitational environment is termed zero gravity in this work. The sides of the drag shield were removable, so that the experiment package could be installed and removed. Prior to deceleration in the sand box, the package came to rest on the bottom of the drag shield, which resulted in a usable zero-gravity test time of 2.25 seconds.

Experiment Package

The experiment package, as shown in figure 4, contained the boiling apparatus, camera and lighting equipment, power supplies, and associated controls.

Figure 5 (p. 12) illustrates pictorially the boiling apparatus. The surface on which boiling was observed was a 0.005-inch-thick, 0.25-inch-wide Chromel strip with an effective heating length of 0.50 inch. The underside of the strip was mounted on an insulating material with high-temperature epoxy resin, while its ends were clamped down between copper blocks. This assembly was mounted on a nonconducting material and enclosed in a glass tube. The tube was designed with a narrow neck at its top to prevent movement of the liquid due to surface tension effects during the transition from normal to zero gravity. Power to the strip was provided by a 4.5-volt, 32-ampere-hour regulated battery supply. The surface was prepared by lapping with number 600 emery paper, polishing with 2/o emery polishing paper, and rinsing with alcohol.

A second heater was mounted in the boiler and used to control the temperature of the bulk of the fluid. Power to this heater was supplied from an alternating-current source external to the experiment package and was turned off prior to a test run.

The bulk fluid temperature was measured by a thermistor mounted on the end of a stainless steel probe. The position of this probe in the boiler, as shown in figure 5, was about 0.5 inch above the test surface and directly over it. A thermistor was also mounted directly beneath the test strip in order to obtain an approximate value for the surface temperature. The resistance of the bulk thermistor was monitored on a digital ohmmeter, while the resistance of the surface thermistor was recorded with an oscillograph.

Heat flux dissipated from the heater strip was determined by measuring the voltage drop across the surface with a vacuum-tube voltmeter. The resistance of the strip was measured accurately prior to testing with a Wheatstone bridge.

The 16-millimeter motion picture camera, equipped with a split frame prism, provided a filming rate of approximately 6500 pictures per second. A 35-millimeter lens,

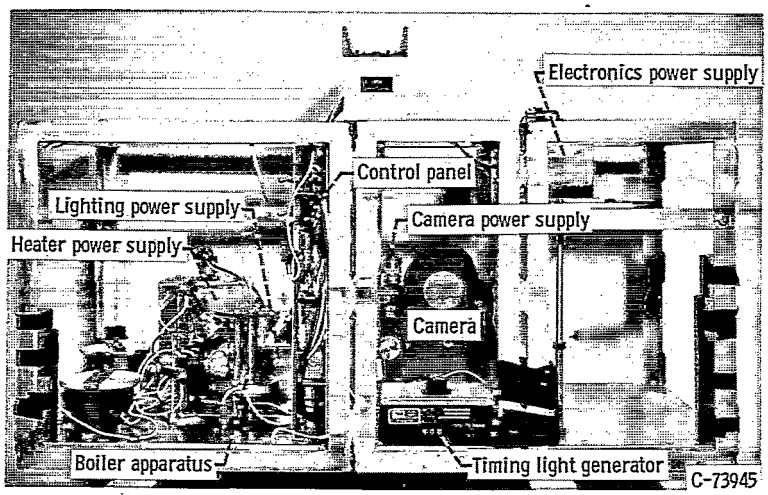

(a) Side view.

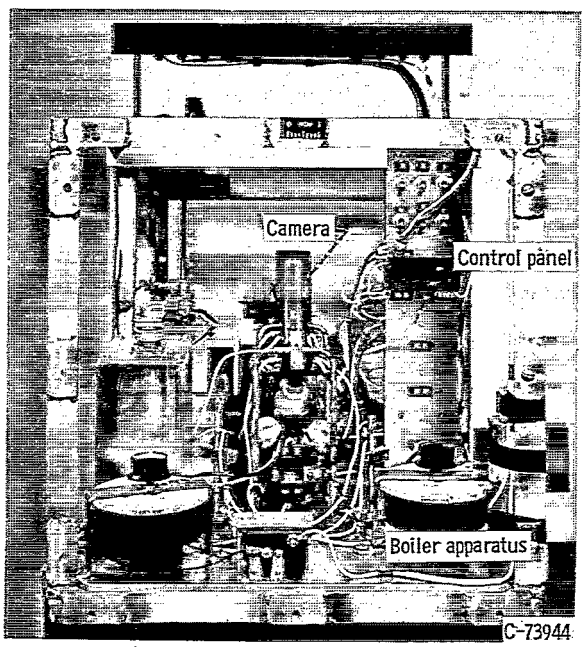

(b) End view.

Figure 4. – Experiment package.

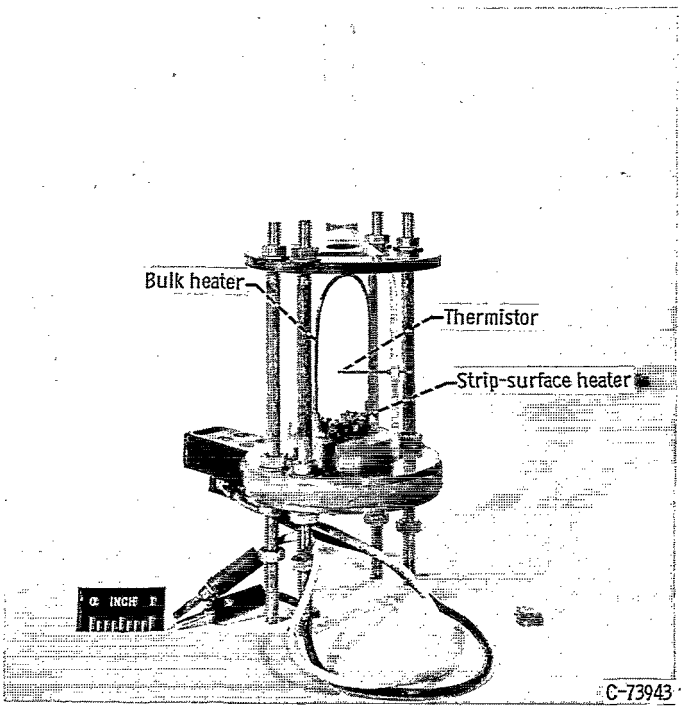

Figure 5. - Boiler apparatus.

set at f4, captured a nominal area 1 inch wide by 0.5 inch high. Timing marks were placed on the film every 1/1000 second by a timing light generator.

Illumination was provided by four 20-watt spotlights located about the boiler in order to produce clear definition of the bubble outlines. The effect of heat from the lamps on the bulk fluid temperature over the approximately 1.25-second test duration was negligible.

EXPERIMENTAL PROCEDURE

The boiler and a 2000-milliliter flask were thoroughly cleaned, flushed with distilled water, and polished. Distilled water was placed in the flask and boiled for 1.5 hours to drive off dissolved gases. The boiler was filled with test fluid from the flask, and the experiment package placed in the drag shield and raised to the top of the drop tower. Power was supplied to the bulk heater, and the water was deaerated further for 15 to 20 minutes.

After the degassing processes were complete, the fluid was permitted to cool naturally, and the bulk temperature was monitored. When the bulk temperature was within 10° F of the desired test temperature, the strip heater was actuated at a level that

initiated boiling. This was done to destroy any stratification that had been set up in the fluid during the cooling period. When the bulk temperature was within 3^{o} to 5^{o} F of the desired test value, the power to the strip heater was increased to the proper level. The heat flux for all experimental runs was approximately 28 900 Btu per hour per square foot. When the digital ohmmeter indicated that the desired bulk temperature was reached, the experiment package was released. The photographic equipment and lights were activated by a system of relays approximately 1 second after release of the package in order to obtain data during the last 1.25 seconds of zero gravity time. Normal gravity testing was the same as that just described for zero gravity, except that when the desired bulk temperature was reached, the camera and lights were activated manually. The procedure was repeated for six bulk temperatures in each gravity field.

The heater surface temperature measurements were made in normal gravity by using the aforementioned procedure. Tests were run for a complete range of subcoolings with a highly polished surface and then repeated for a slightly polished one. The reason for testing heaters that had different surface conditions is discussed later in the report.

DATA REDUCTION

The bubbles recorded on the 100-foot rolls of film were viewed and measured on a motion analyzer that magnified the image eight times. Measurements on a bubble were made with the assumption that a vertical cross section was being viewed. In order to determine the position of the bubbles on the surface, however, the camera was inclined at approximately 5^{o} from the horizontal so that a small error was present in the data. Inclination of the camera permitted selection of bubbles that were generated in the center of the heater and, hence, free of possible effects from the heater edges.

In order to analyze the growth characteristics of bubbles statistically, lifetime, time during which a bubble is attached to a surface, and maximum radius were tabulated for as many as 15 bubbles at each subcooling and gravity level. Only those bubbles that grew undisturbed on the surface were used, so that under some conditions, fewer than 15 were available.

The force analysis was applied to a minimum of two bubbles at each subcooling and gravity level. Calculations were performed by a computer because of the large volume of work required. The derivatives required in equations (8) and (12) were obtained by the computer first fitting the second through tenth degree curves to the data points. Then, the curve that best represented the data was placed in the computer, which calculated the slope of the curve at the necessary points.

Force histories, plots of force against time, were prepared for the individual bubbles so that the stimulus for removal could be studied. Force comparisons between

bubbles were made by a nondimensional technique in which each positive force was divided by the total positive force and actual time was divided by lifetime. Plots of a particular dimensionless force against dimensionless time were made for bubbles at different subcoolings and gravity levels. Because of the large amount of information generated from the procedures just described, only a representative cross section of the force data is presented in this work.

Further analysis involved the selection of a critical point at which the removal forces imparted enough inertia to a bubble to start separation. This point was defined as that time during bubble collapse when the inertia of the bubble vapor, or the net force on the bubble, reached a maximum positive value; however, it was stipulated that the time selected should not occur during the last moments of the lifetime. These last moments were characterized by a rapid decrease in the bubble base diameter, so that the large positive inertia exhibited by some bubbles at that time was believed to be caused by, rather than the cause of, the impending separation. The values of the different dimensionless forces at the critical point were plotted against subcooling for normal and zero gravity.

RESULTS AND DISCUSSION

Determination of Surface Tension

In order to calculate the surface tension force from equation (3), it was necessary to determine the surface tension at the heater surface. Because surface tension is a function of temperature, the heater surface temperature was measured. These temperature measurements were made in normal gravity, and the resulting calculated surface tension was used in both the normal and zero gravity force calculations. It is not to be inferred that the surface temperatures are not a function of gravity but rather that there may be some degree of error in the associated zero gravity calculations. The formula for the surface tension as a function of temperature was obtained from reference 25.

The data obtained from these measurements are presented in figure 6. Each data point represents an average temperature taken over approximately 15 to 20 seconds. An average was used because the actual temperature fluctuated, as shown by a typical oscillograph trace in figure 7. Previous investigators such as Chun (ref. 11) and Han and Griffith (ref. 12) have indicated that boiling is dependent on the condition of the heater surface. Therefore, the heaters used for these tests were prepared so that their surface conditions were extremes of the surface conditions used in the photographic tests. In figure 6, curve I represents data for the extensively polished surface, while curve II is data taken for the slightly polished one. As expected, the rougher surface produced

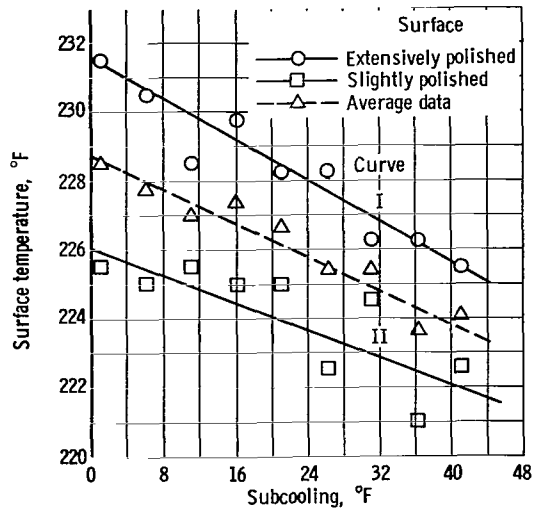

Figure 6. - Effect of surface conditions and subcooling on surface temperature. Average heat dissipation maintained at 28 900 Btu per hour per square foot.

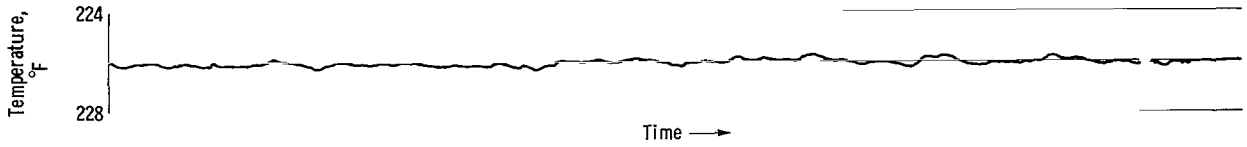

Figure 7. - Fluctuation of surface temperature.

cooler temperatures because of the more numerous nucleation sites. The surface temperatures used to obtain the surface tension were taken from an average of the data points. The trend toward higher surface temperatures for higher bulk temperatures in the low heat flux region is also noted in reference 20.

Bubble Growth Characteristics

Investigation of the motion picture films indicated that the shape of the bubbles deviated considerably from spherical for most test conditions. This was expected from the results of references 18 and 19. However, an exception to this occurred at the high bulk temperatures, where smaller bubbles appeared to be more spherical. These results are due to the existence of a thermal growth layer adjacent to the heater surface and over which the temperature decreases from the heater surface temperature to the saturation temperature. The thickness of the layer can be such that all the bubbles observed, except the smaller ones at low subcoolings, extend out of the layer into the subcooled liquid. This causes condensation on the top surfaces of the bubbles, so that their shape

deviates from spherical. The fact that the smaller bubbles at low subcoolings were not distorted by condensation suggests that the thermal growth layer was thicker under such conditions.

The bubbles observed were of two types: continuous growth, in which the volume of the bubbles increased, reached a maximum, and then decreased until separation from the surface occurred; and, oscillatory, in which the volume of the bubbles went through several cycles of first increasing and then decreasing volume before separation from the surface occurred. These types of bubbles have also been observed by the University of Denver (refs. 18 and 19). At the low bulk temperatures, all the bubbles were of a continuous growth type in both zero and normal gravities, and there was little coalescence noticeable between adjacent bubbles. As the saturation point was approached, oscillator-type bubbles began to appear, particularly in zero gravity. There was occasional coalescence in normal gravity and extensive coalescence in zero gravity. Figure 8 presents interrupted photographic sequences of bubbles growing at approximately 38^{o} and 5^{o} F subcooling in both normal and zero gravity. The sequences are considered typical of the particular boiling conditions.

As has been observed in reference 3 separation of the bubbles did not occur always at the heater surface; it occurred often a short distance above the surface on a shrinking neck, and a residue was left to form a new bubble. After leaving the surface, the bubbles that were generated at high subcooling at both gravity levels rapidly moved into the liquid bulk and condensed. In normal gravity near saturation, the bubbles left the surface more slowly than at high subcooling and did not condense within the field of view of the camera. In contrast, for low subcoolings in zero gravity, the bubbles barely separated; some returned to the surface before rising into the bulk. Several of the larger coalescing bubbles separated and moved so slowly into the bulk that subsequent bubbles forming on the heater surface were absorbed into the rising vapor mass. This latter phenomena is proposed as a principal heat-transfer mechanism in reduced gravity in reference 3.

Further zero-gravity tests as close to the saturation point as possible indicated a large vapor mass situated above the heater strip into which the generated vapor from the surface was absorbed. As time progressed, the vapor mass surrounded the heater, and burnout seemed imminent. The primary difference, then, between saturated and slightly subcooled conditions in zero gravity was not separation of the bubbles but the inability of the vapor under saturated conditions to be removed from the vicinity of the heater surface. These results indicate the time dependence of burnout in zero gravity under saturated conditions, as proposed by Clodfelter (ref. 7).

Bubble population decreased in both gravity levels as the bulk temperature was increased. Rough counts of the total number of bubbles generated over the test durations showed a moderate population decrease in normal gravity as compared with a considerable decrease in zero gravity.

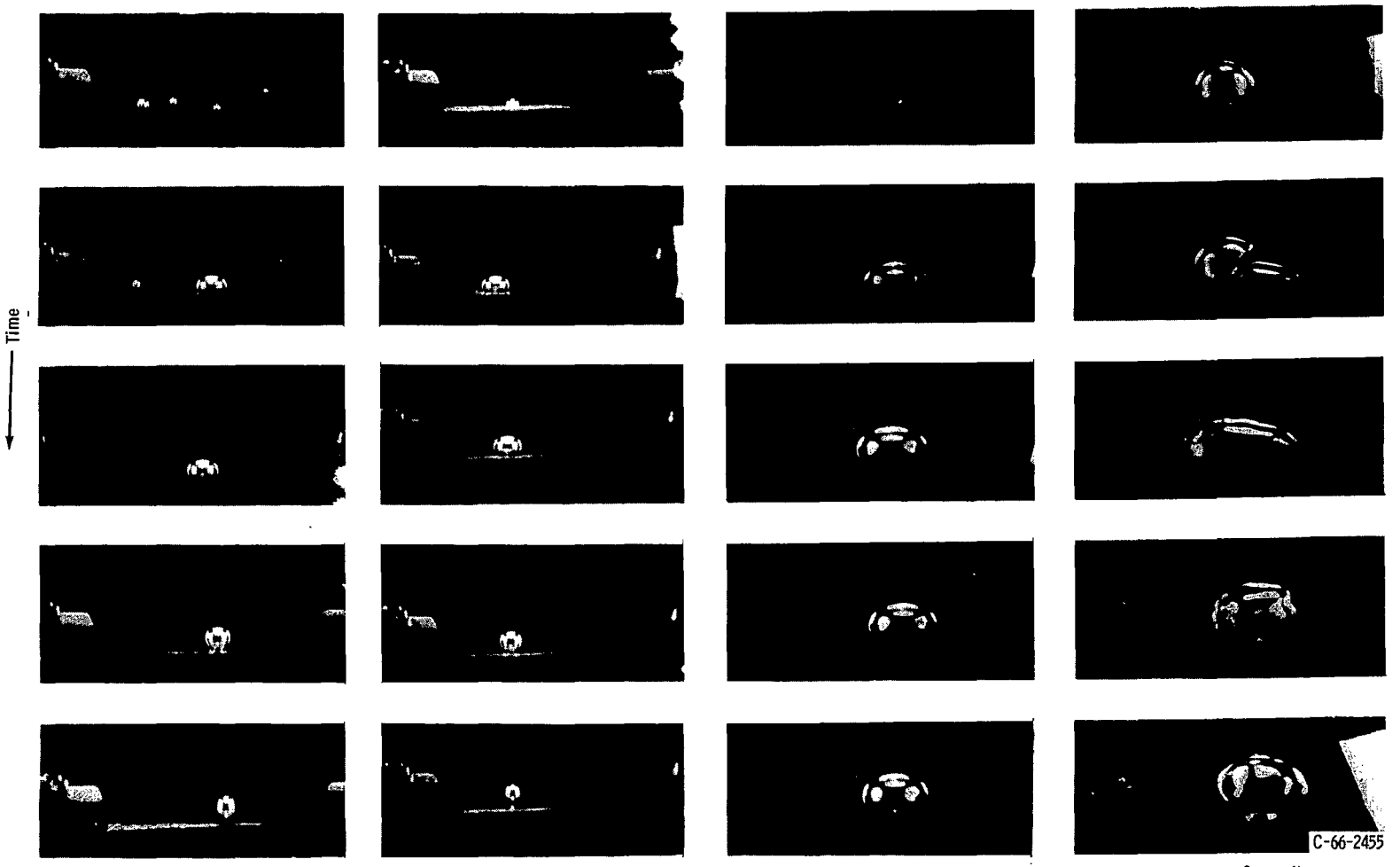

(a) Subcooling, 38.6°; gravity, normal. (b) Subcooling, 38.5°; gravity, zero. (c) Subcooling, 5.1°; gravity, normal. (d) Subcooling, 4.4°; gravity, zero.

Figure 8. - Bubble growing on heated surface.

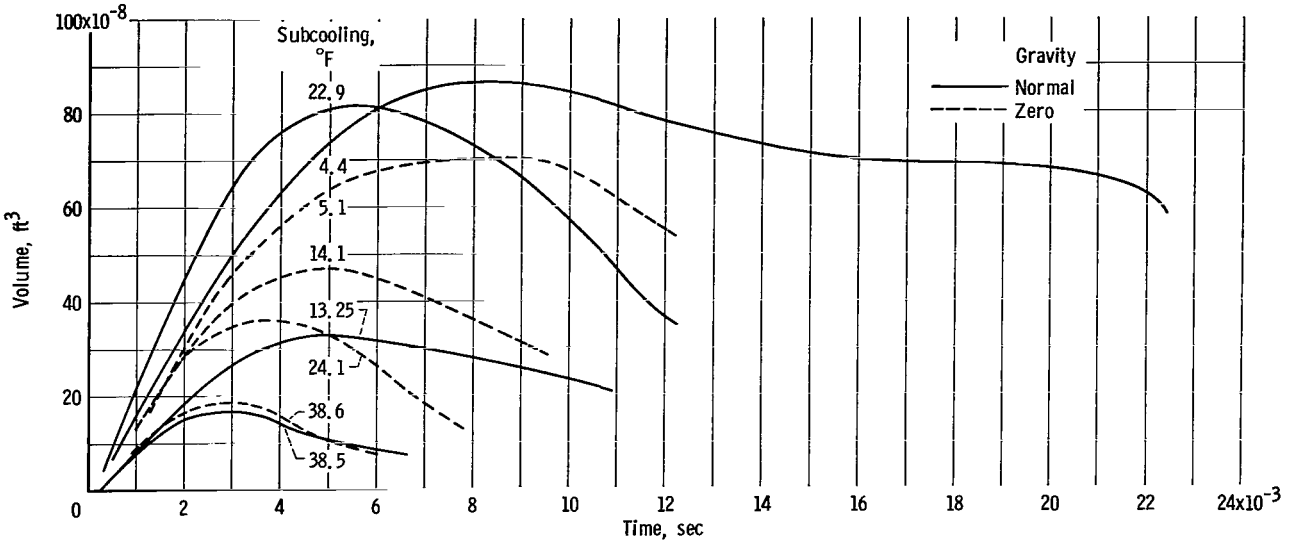

Figure 9. - Growth of bubbles at various subcoolings.

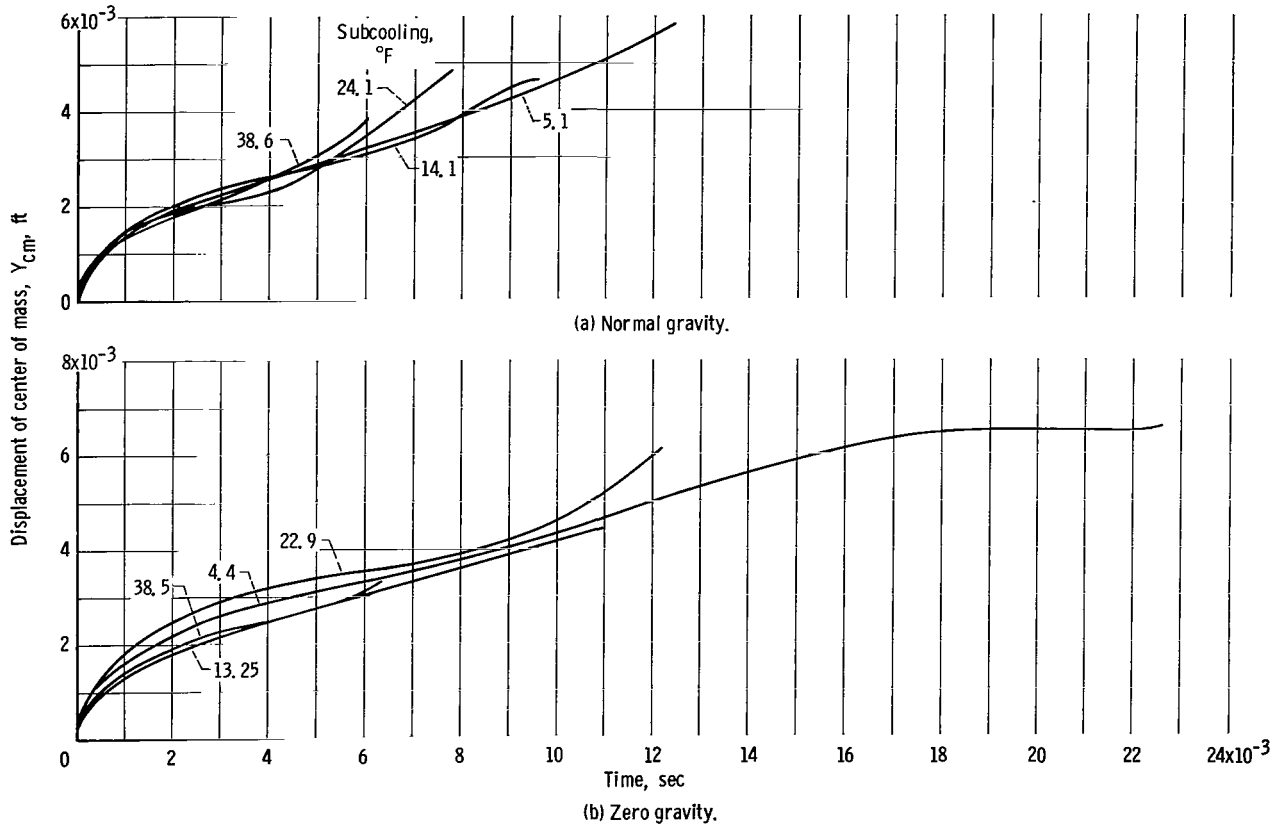

Figure 10. - Rise of center of mass of bubbles at various subcoolings in normal and zero gravity.

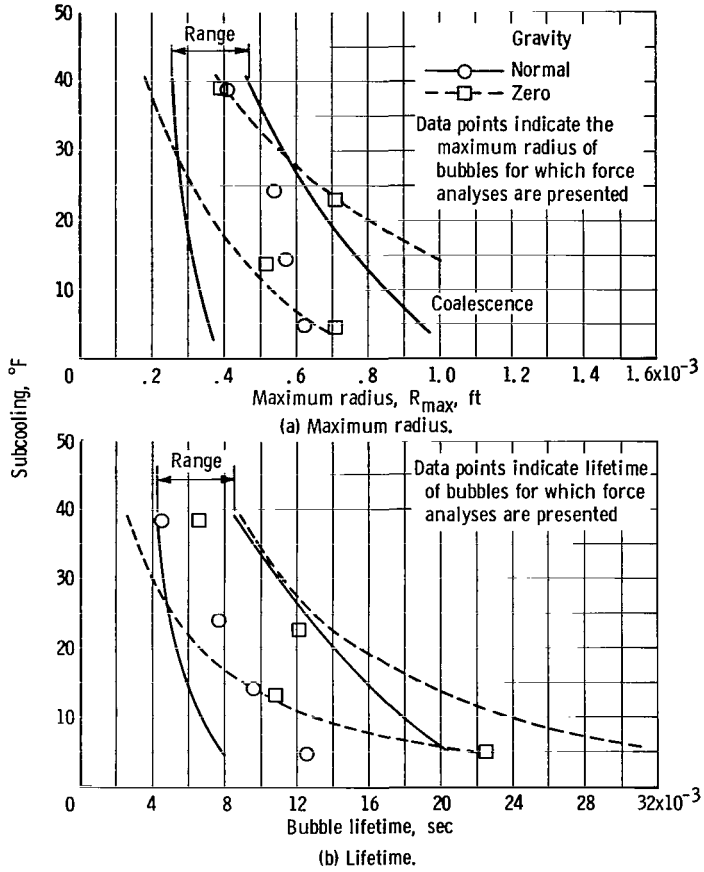

Figure 11. - Effect of subcooling on bubble maximum radius and lifetime.

Plots of total volume against time and center of mass against time are presented in figures 9 and 10, respectively. It is apparent from figure 9 that the bubble lifetimes were divided into two periods, growth and collapse, and from figure 10 that the translations of the centers of mass attained greater rates early in the lifetimes when the bubbles grew rapidly.

The change in the maximum bubble radius with subcooling and gravity level is shown in figure 11(a). The data points represent the maximum radii of bubbles for which force histories and dimensionless data are presented later in this report. It can be seen that a range of bubble sizes was observed at any one subcooling in both gravity levels; a trend toward larger bubbles was evident at higher bulk temperatures. A comparison of normal and zero gravity data indicates that, at high subcooling, comparable values were obtained. As the bulk temperature was increased, the maximum radii in zero gravity became larger than those for normal gravity except for very low subcooling. The discrepancy at low subcooling was caused by the aforementioned coalescence, the result being that only smaller bubbles were able to grow undisturbed. The trend toward larger bubbles at

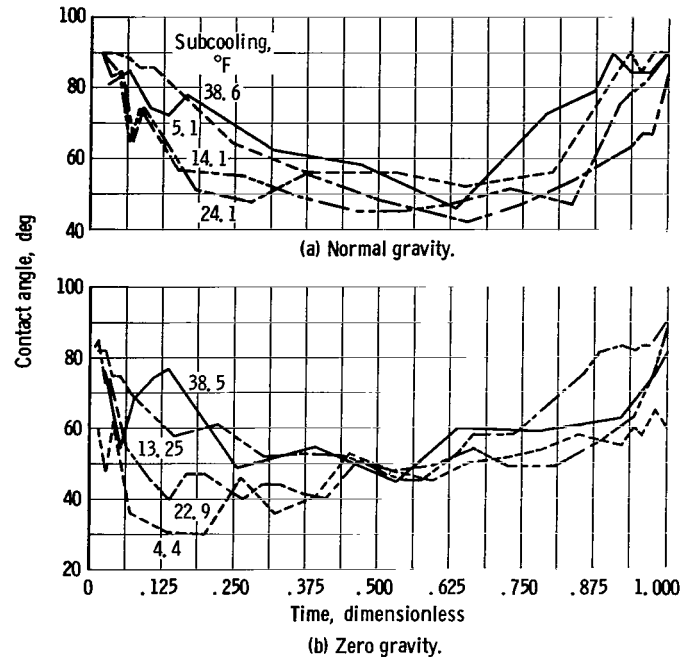

Figure 12. - Variation of bubble dynamic contact angle with time for various subcoolings in normal and zero gravity.

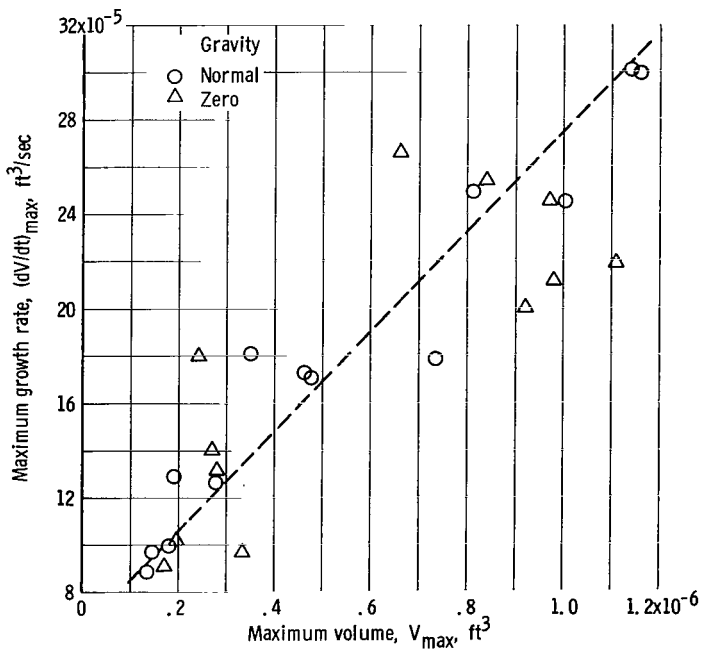

Figure 13. - Variation of bubble maximum growth rate for normal and zero gravity.

lower subcoolings substantiates the theory of a thicker thermal growth layer at increasing bulk temperatures.

Data for bubble lifetime as a function of subcooling and gravity level exhibit much the same trends as do the maximum radius data, as shown in figure 11(b) (p. 19). It is notable that, even though the lifetimes of only the smaller bubbles were measured at low subcooling and zero gravity, the increasing lifetime trend continues as subcooling decreases.

The change in the dynamic contact angle with dimensionless time is shown in figure 12 for several bubbles. The bubbles initially formed with high contact angles, approaching 90^{o}, decreased with increasing volume, and then increased to 90^{o} again at separation. The trend toward higher angles as separation is approached has been observed by several investigators. It was difficult to measure this angle, and it is estimated only to be within 10^{o} of the true value. No clear trend regarding gravity dependence was evident.

The time rate of change of the volumes of bubbles, or growth rate, shows a trend to higher positive maximum growth rates for larger bubbles, as shown in figure 13. Therefore, from figure 11(a) (p. 19), a range of maximum growth rates may be expected at each subcooling and gravity level, and a trend toward higher maximum growth rates for lower subcoolings and zero gravity is predicted.

Graham and Hsu (ref. 10) have proposed the dependence of bubble growth rate on the thermal layer thickness. Since previous findings in this work indicated that the thickness of the thermal growth layer increased as subcooling decreased and gravity level was reduced, the trend in the maximum growth rates may be explained. The maximum growth rate was attained very early in the bubble lifetime, as has been proposed by Han and Griffith (ref. 12).

A summary of the previous discussions involving the effects of subcooling and zero gravity on bubble characteristics is presented in table I (p. 22).

Discussion of Forces

Effect of subcooling in normal gravity. - Examination of the force histories in figure 14 (pp. 23 and 24) shows that the general shapes of the pressure force and surface tension force curves did not change with subcooling. The magnitudes, however, did become larger as the subcooling was decreased because of the increased size of the bubbles. It should be noted that different scales were used on plots at different subcoolings in order to make the data presentation clearer. Investigation of the dimensionless plots in figures 15(a) and 16(a) (pp. 25 and 26, respectively) shows that the pressure force accounted for a large percentage of the total removal force at the critical point (see p. 14) for all subcoolings.

TABLE I. - EFFECTS OF INCREASING SUBCOOLING AND ZERO GRAVITY ON BUBBLE CHARACTERISTICS

Characteristic	Effect of increasing subcooling on bubble characteristics		Effect of zero gravity on bubble characteristics	
	Gravity		Subcooling	
	Normal	Zero	High	Low
Coalesence of adjacent bubbles	Decreased from occasional to little or none	Decreased from extensive to little or none	No apparent effect	Increased from occasional to extensive
Type of bubbles	Continuous growth and few oscillators to just continuous growth	Continuous growth and many oscillators to just continuous growth	Continuous growth for both gravity levels	Continuous growth and few oscillators to continuous growth and many oscillators
Bubble population	Moderate increase	Considerable increase	Slight decrease	Considerable decrease
Bubble maximum radius	Decreased	Decreased	No apparent effect	Increased
Bubble lifetime	Decreased	Decreased	↓	Increased
Contact angle	No apparent effect	No apparent effect		No apparent effect
Maximum growth rate	Decreased	Decreased		Increased

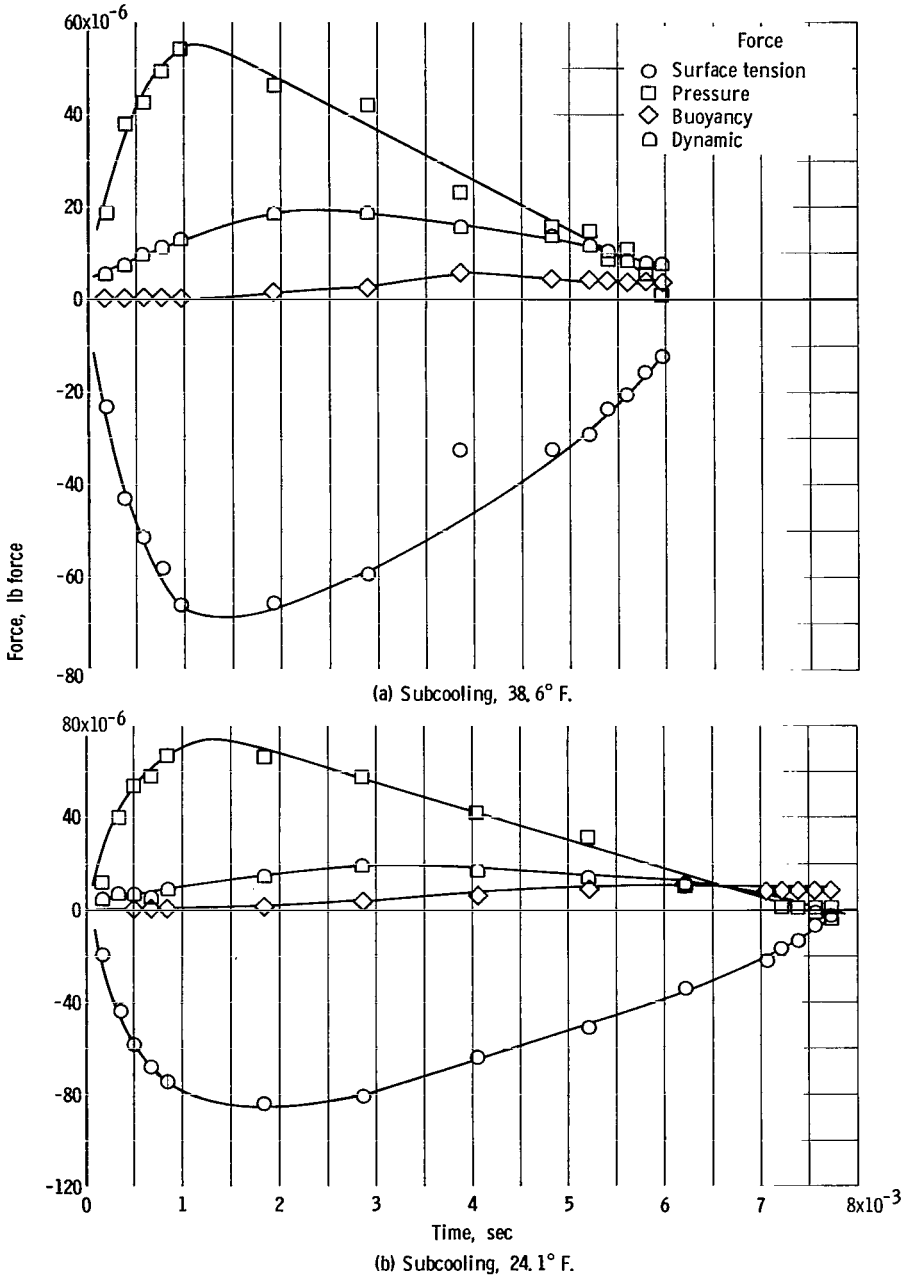

(a) Subcooling, 38.6° F.

(b) Subcooling, 24.1° F.

Figure 14. - Dynamics of bubble at various subcoolings and normal gravity.

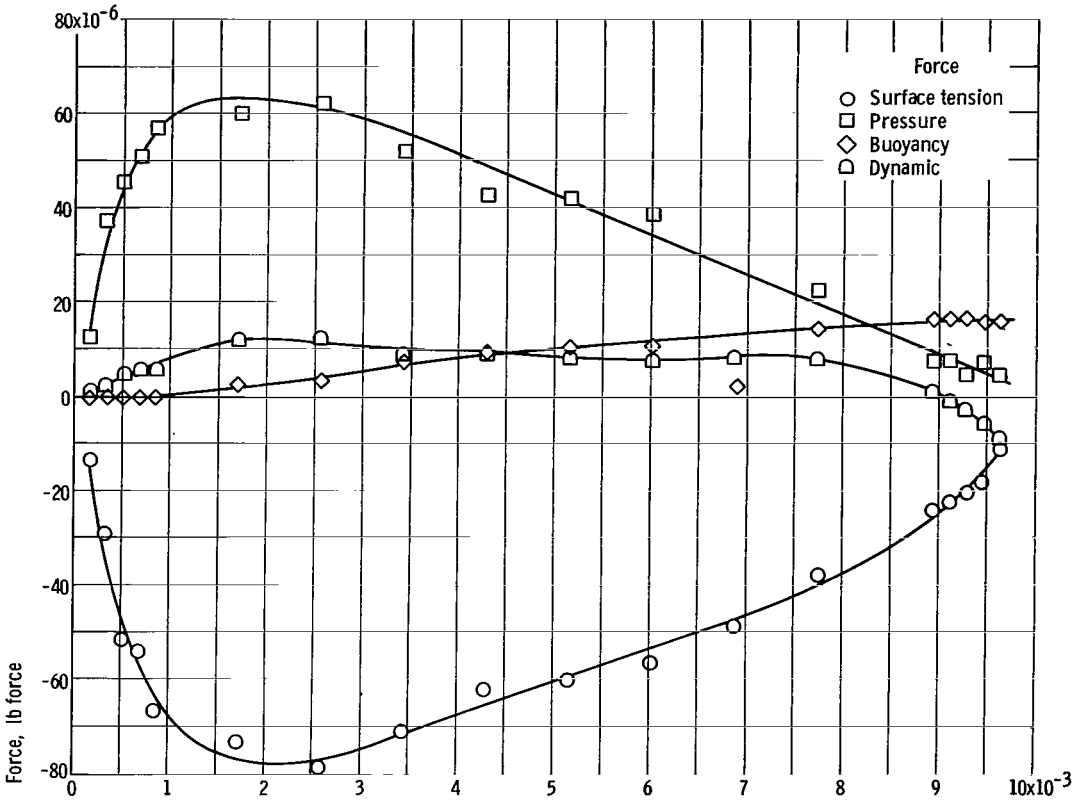

(c) Subcooling, 14.1° F.

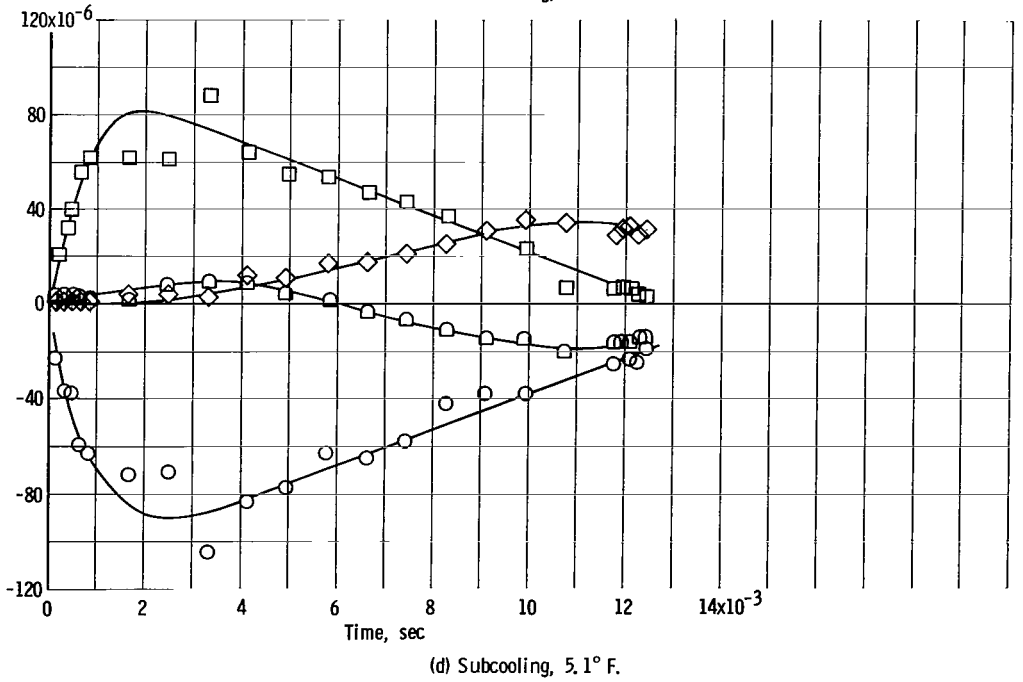

(d) Subcooling, 5.1° F.

Figure 14. - Concluded.

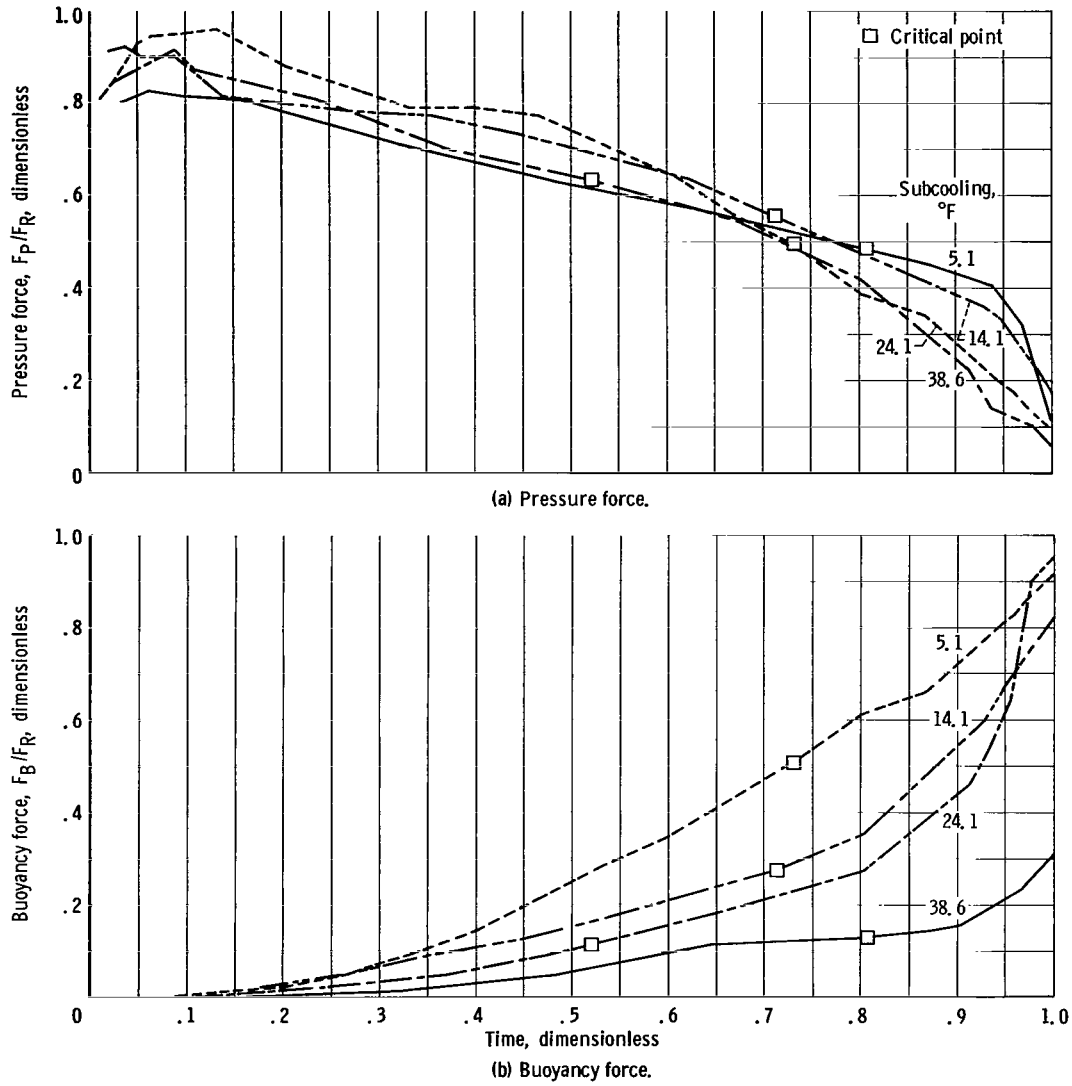

(a) Pressure force.

(b) Buoyancy force.

Figure 15. - Effect of buoyancy and pressure forces on bubble dynamics at various subcoolings in normal gravity.

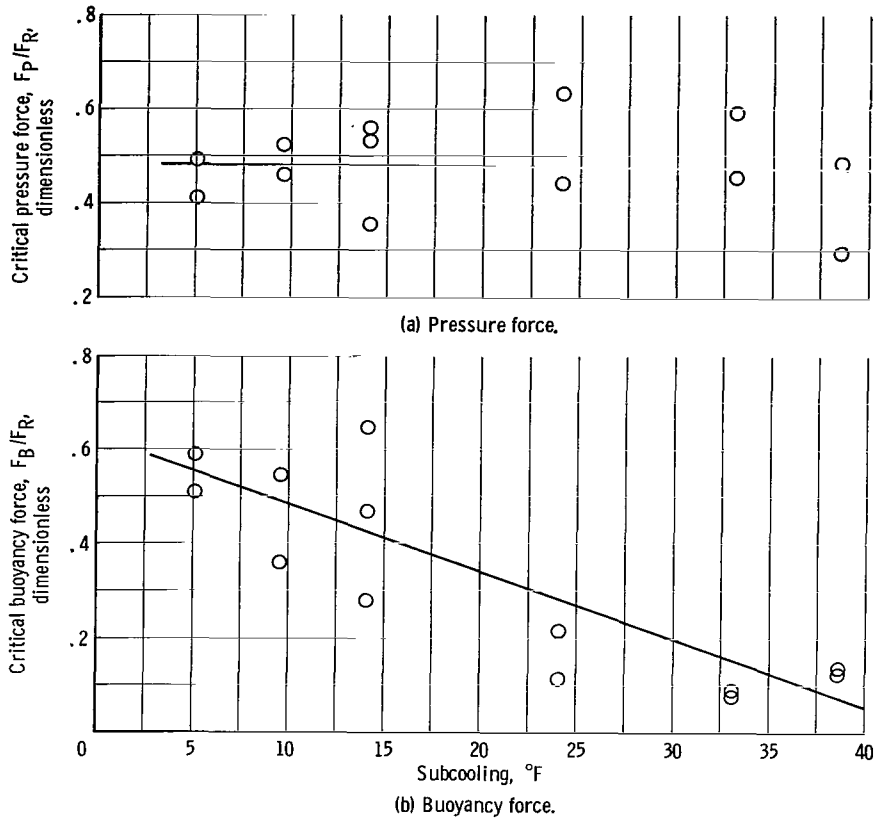

Figure 16. - Effect of pressure and buoyancy forces on bubble separation at various subcoolings in normal gravity.

The effect of subcooling on the buoyancy force could have been predicted from the maximum radius curves in figure 11 (p. 19). The dimensionless plots in figures 15(b) and 16(b) indicate the greater importance of buoyancy as the subcooling was decreased; at the critical point, buoyancy accounted for a major percentage of the total removal force for low subcooling as compared with a small percentage for high subcooling.

The drag force is not shown on the force histories because it was very small; this force accounts for a maximum of about 4 percent of the total retention force. The existence of this force as defined herein may be questioned if a source flow model for the fluid flow about the bubble, as has been proposed by Zuber (ref. 24), is assumed. For such a model, the liquid around the bubble flows radially away from the nucleation site.

The role that the dynamic force played in the removal of bubbles was highly dependent on subcooling, as shown in figure 17. At the critical point, it diminished from a major percentage of the removal force at high subcooling to insignificance and retardation at low subcooling. This retentive dynamic effect may account for differences that have been found between theoretical and experimental results regarding bubble size at departure. While investigating at approximately the saturation point with water, Siegel

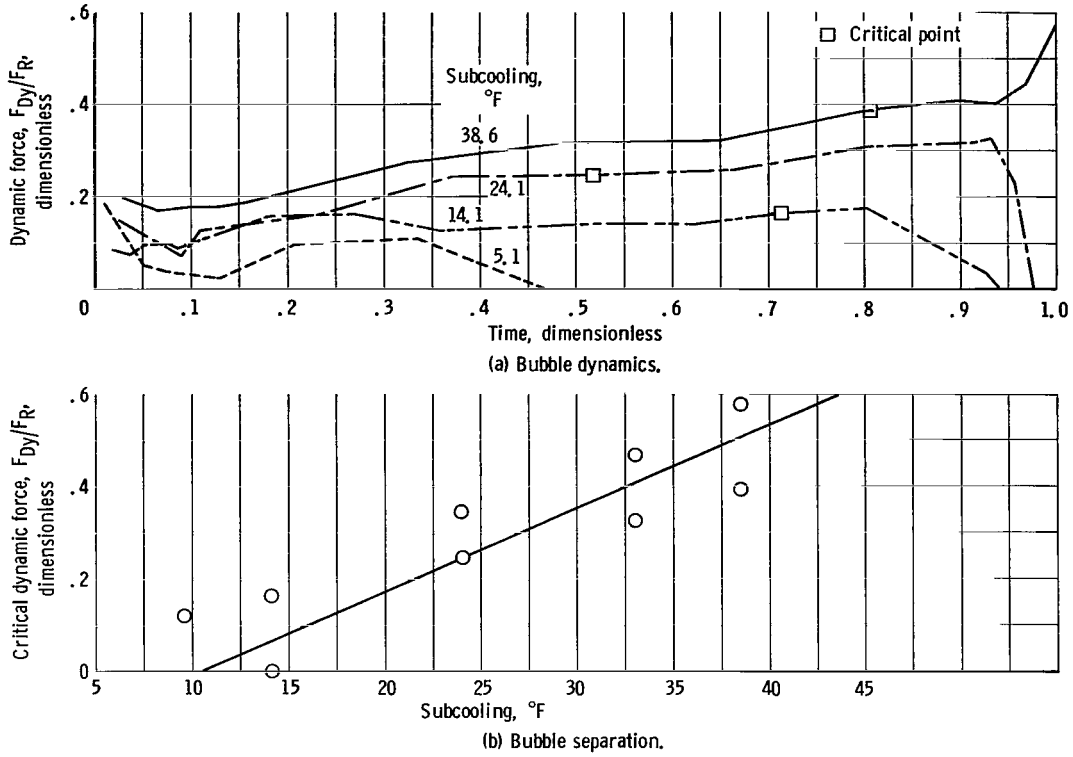

Figure 17. - Effect of dynamic force on bubble dynamics and bubble separation at various subcoolings in normal gravity.

and Keshock (ref. 3) found discrepancies between their experimental results and those predicted by Fritz's theory (ref. 26), an equation derived from the equivalence of surface tension and buoyancy. They determined that the experimental diameters were as much as 20 percent greater than Fritz's diameters, which indicates that something retained the bubbles for additional growth. Another equation for bubble size at departure, derived by Staniszewski (ref. 27), included a retentive dynamic term.

In summary, in normal gravity bubbles generated at high subcooling were removed principally by the pressure and dynamic forces with buoyancy playing a minor role, while at low subcooling the stimulus for bubble removal was the pressure and buoyant forces with the dynamic force acting retentively. The drag force was negligible; surface tension accounted for the retention force for all subcoolings.

Effect of gravity level at various subcoolings. - The zero gravity force histories in figure 18 (pp. 28 and 29) indicate that the surface tension and pressure forces acted much the same as in normal gravity. Investigation of the dimensionless plots for the pressure force in zero gravity in figures 19(a) and 20(a) (pp. 30 and 31, respectively) shows that this force accounted for a large percentage of the total removal force at the critical point for all subcoolings. Comparison of the zero gravity curve with the normal gravity curve

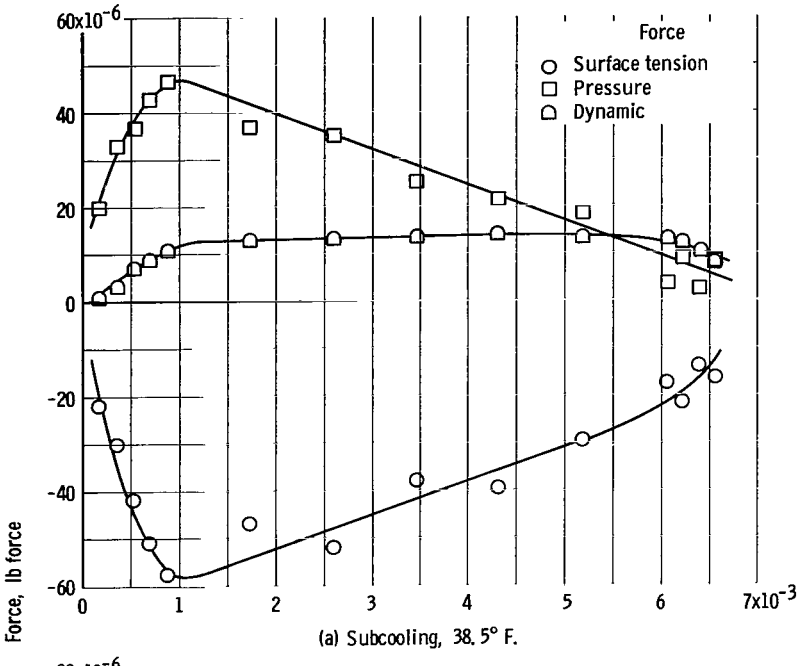

(a) Subcooling, 38.5° F.

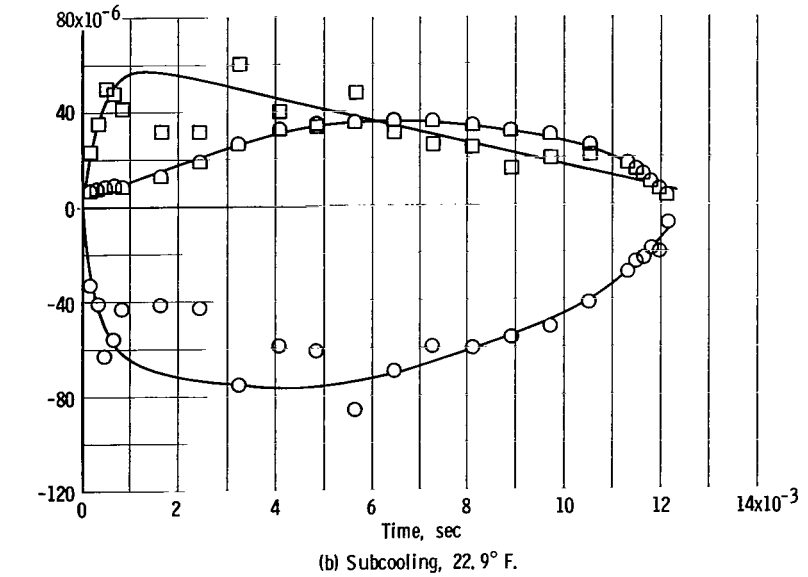

(b) Subcooling, 22.9° F.

Figure 18. - Dynamics of bubble at various subcoolings and zero gravity.

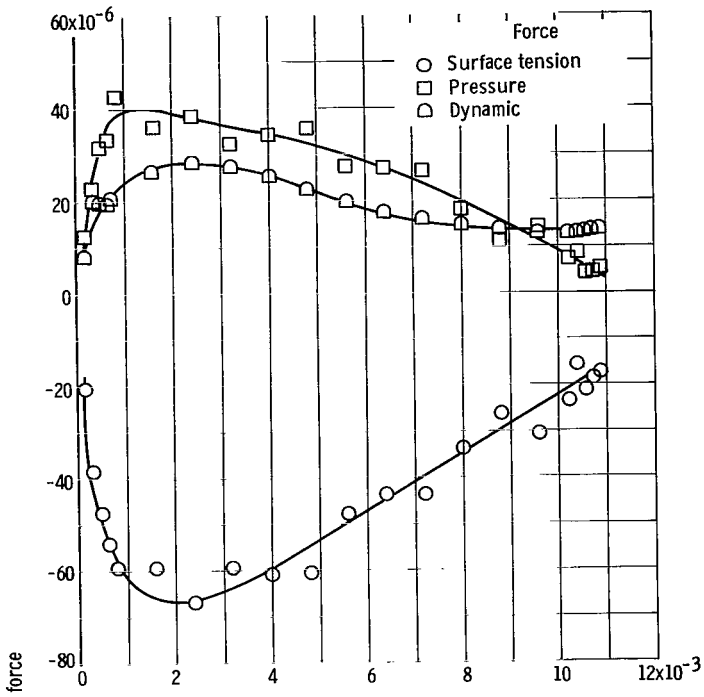

(c) Subcooling, 13.25° F.

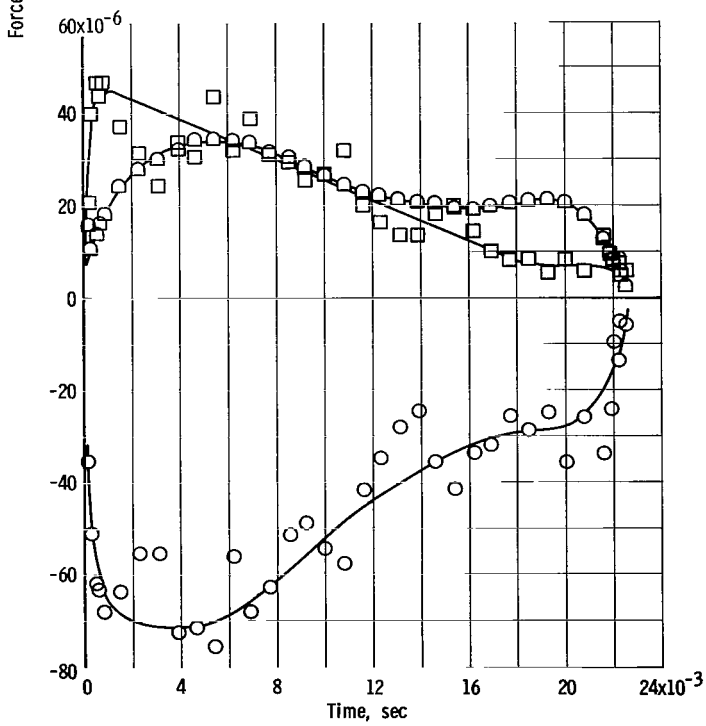

(d) Subcooling, 4.4° F.

Figure 18. - Concluded.

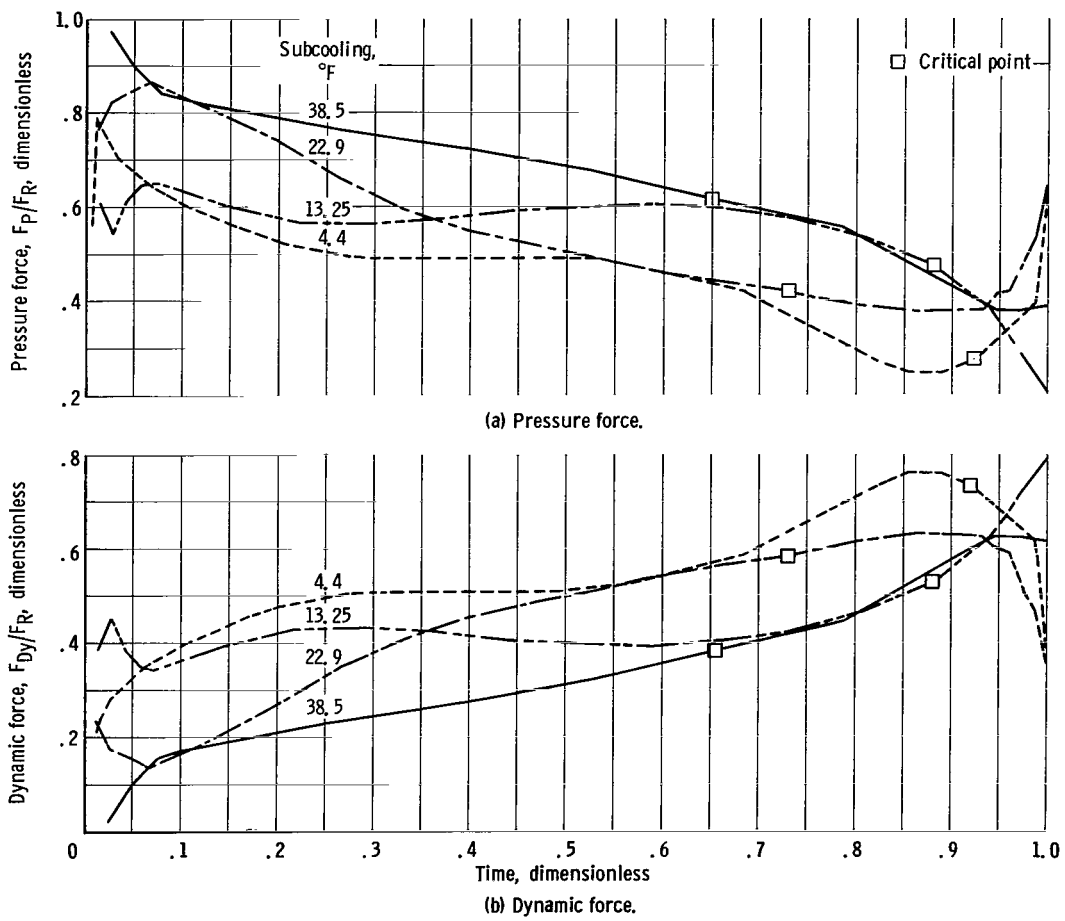

Figure 19. - Effect of pressure and dynamic forces on bubble dynamics at various subcoolings and zero gravity.

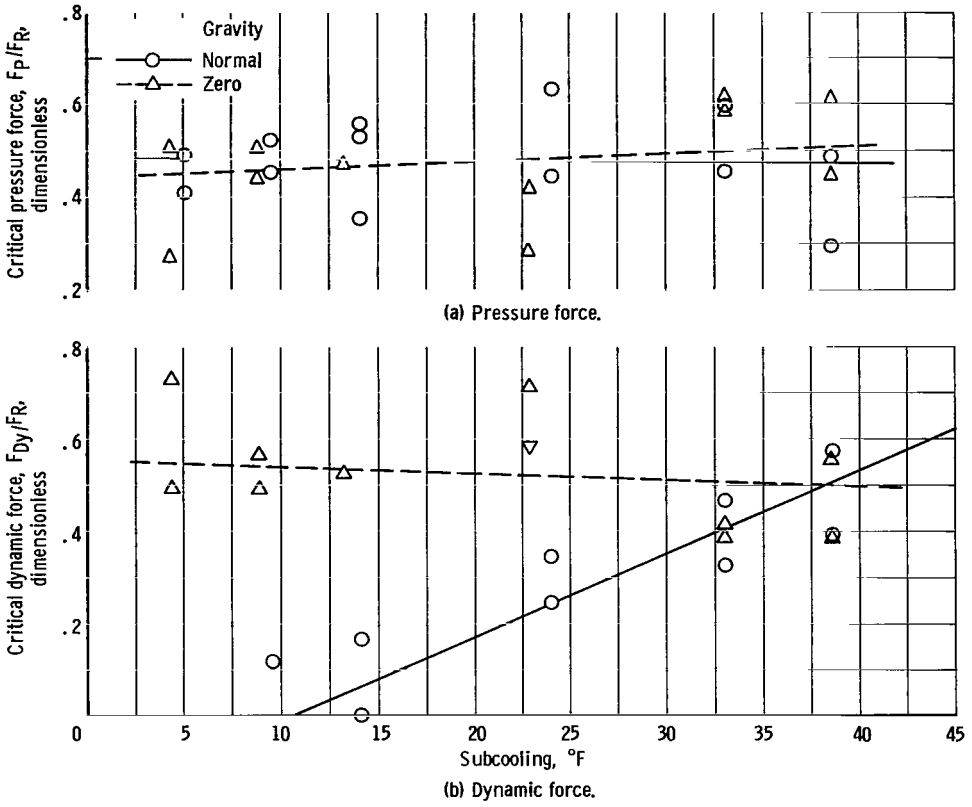

Figure 20. - Effect of pressure and dynamic forces on bubble separation at various subcoolings in normal and zero gravity.

in figure 20(a) indicates that the pressure force was not affected by the reduction in gravity.

The dimensionless plots in figures 19(b) and 20(b) and the zero gravity force histories show the important role that the dynamic force assumed at the critical point for all subcoolings. At high subcooling, the role that the dynamic force assumed in bubble removal was comparable at both gravity levels, whereas at low subcooling it was not. It is reasonable to assume that, in order to effect bubble removal at low subcooling, the pressure and/or dynamic force assumed a more important role in zero gravity to make up for the absence of the buoyancy force.

In zero gravity, therefore, the pressure and dynamic forces removed the bubbles at all subcoolings, and surface tension accounted for the retentive force.

Dynamic Force Discussion

In an analysis of the motion of a bubble generated on a heated surface, it is

necessary to recognize the existence of a force applied to the vapor mass and caused by the effect of the surrounding liquid set in motion by the growing and collapsing bubble. A search of the literature did not yield a formulation which described the phenomena accurately. In this report, Newton's second law of motion was applied to the bubble, and the unknown force, termed the dynamic force, was determined from the measured vapor inertia terms and the other identified forces (see eq. (12), p. 7). In this approach to the problem, the dynamic force term implicitly contained all the terms necessary to satisfy the equation of motion. Although the method of formulation yielded the magnitude of the dynamic force, it did not provide explicit information regarding the cause or causes of the force. It should also be noted that the applicability of this approach during the early portions of the bubble lifetime may be questioned. At this time, the growth rate of the bubble was very high, and the motion of its center of gravity away from the surface may have been dominated by the growth of the bubble in the thermal layer rather than the result of positive applied forces.

In considering the causes of the dynamic force, it is believed that the bulk of this force is associated with the momentum of the liquid surrounding the vapor; thus, a discussion of the liquid flow fields is necessary. A flow similar to a source type, as proposed by Zuber (ref. 23), occurred for the growth portion of the bubble lifetime. This is illustrated by the bubble profiles in figure 21(a), where it can be seen that the liquid-vapor interface continually moved away from the nucleation site. During collapse of the bubble, a source type of flow existed near the top of the bubble, where the liquid-vapor interface was still moving away from the nucleation site. Near the heater surface, however, because the bubble base was decreasing, a flow toward the nucleation site (a sink flow) was occurring, as shown in figure 21(b).

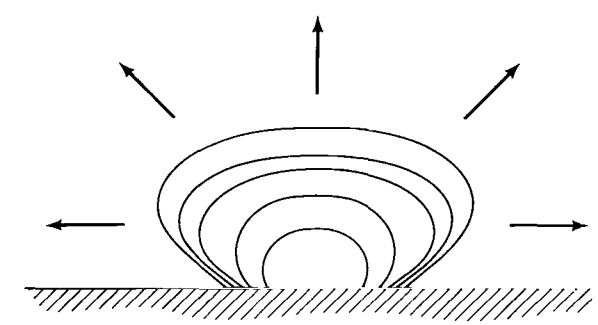

(a) Bubble growth.

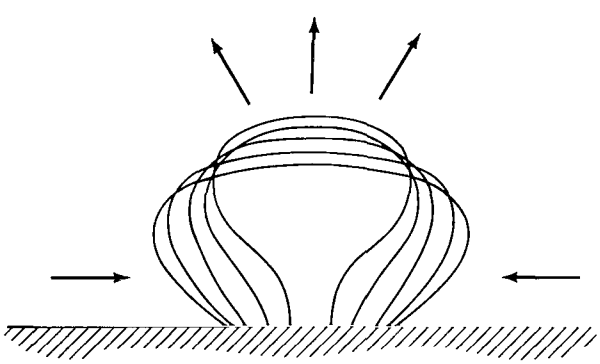

(b) Bubble collapse.

Figure 21. - Profiles of bubble at 22.9° subcooling and zero gravity illustrating liquid flow patterns.

The mechanism by which the momentum of the liquid affects the bubble has not been determined exactly. A proposal for this mechanism, made by Han and Griffith (ref. 12), suggests that the momentum imparted to the liquid ahead of the bubble tends to draw the bubble off the surface if the growth of the bubbles decelerates

rapidly enough. During bubble growth, therefore, the liquid source flow and the evidence that the growth rate decreased rapidly provide support for this theory. Han and Griffith's proposed mechanism also partially applies during collapse because of the source flow occurring at the top of the bubble. However, the sink flow near the heater surface gives rise to a different mechanism, one that is caused by dynamic pressure on the bottom portion of the liquid-vapor interface.

SUMMARY OF RESULTS

An analysis of the dynamics of a bubble generated on a flat surface resulted in a new formulation for the pressure, buoyancy, and dynamic forces. Application of the analysis to experimental data taken from high-speed motion pictures of boiling water at low heat flux and various subcoolings in normal and zero gravity indicated the following results:

1. The newly defined pressure force was of major significance and accounted for a large percentage of the total removal force at the critical point for all subcoolings and gravity levels.

2. In the discrete bubble region at high subcooling, the pressure and dynamic forces as defined herein were the primary stimuli for removal in both normal and zero gravities; this accounts for the gravity-independent nature of boiling phenomena exhibited at such conditions.

3. At low subcooling, the importance of the dynamic force in bubble removal increased in zero gravity as compared with normal gravity, which makes up for the absence of the buoyancy force and, hence, aids bubble removal.

4. The drag force is of minor importance in the retardation of bubbles growing on a surface.

Observation of boiling at the various test conditions and measurements of bubble characteristics resulted in the following conclusions:

1. The thermal growth layer thickness appeared to be a function of subcooling and gravity level, except at high subcooling, where the layer seemed to be independent of gravity level.

2. Continuous-growth bubbles were generated at all subcoolings and gravity levels, and some oscillatory bubbles appeared as subcooling was decreased in normal and zero gravities.

3. Bubble maximum radius and lifetime were functions of subcooling and gravity level, except at high subcooling, where they were independent of gravity level.

4. The bubble dynamic contact angle approached 90° at bubble inception and separation and did not appear to be affected by subcooling and gravity level.

5. The growth rate of a bubble reached a positive maximum early in its lifetime and appeared to be a function of the thermal growth layer thickness.

6. In zero gravity when the liquid temperature was close to the saturation point, the generated vapor lingered in the vicinity of the heated surface.

Lewis Research Center,
National Aeronautics and Space Administration,
Cleveland, Ohio, June 8, 1966,
124-09-03-01-22.

APPENDIX A

BUOYANCY FORCE CALCULATIONS

The net upward differential pressure force acting on the differential bubble surface areas, as shown in figure 22, is

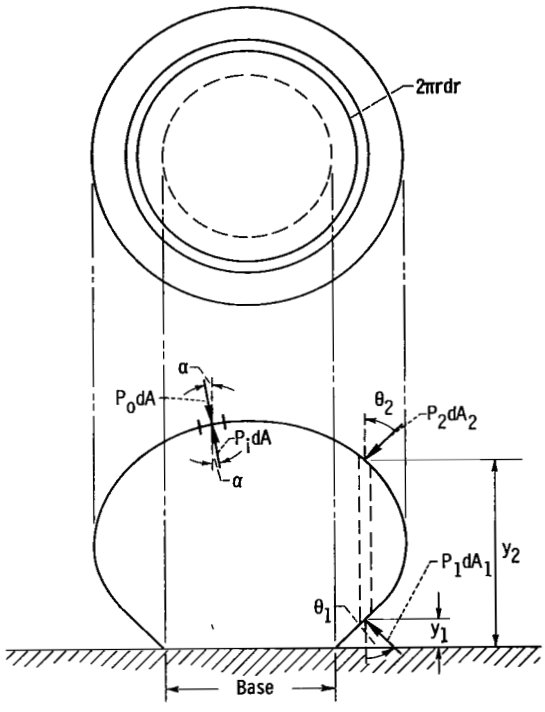

Figure 22. - Bubble schematic.

$$dF_B = P_1 \cos \theta_1 \, dA_1 - P_2 \cos \theta_2 \, dA_2 \qquad \text{(A1)}$$

However,

$$\cos \theta_1 \, dA_1 = \cos \theta_2 \, dA_2 = 2\pi r \, dr \qquad \text{(A2)}$$

and

$$P_1 - P_2 = \rho_\ell \frac{g}{g_c} \left(y_2 - y_1\right) \qquad \text{(A3)}$$

Substituting equations (A2) and (A3) in (A1) yields

$$dF_B = \rho_\ell \frac{g}{g_c} \left(y_2 - y_1\right) 2\pi r \, dr \qquad \text{(A4)}$$

Integrating over the surface area that is not directly over the base results in

$$F_B = \rho_\ell \frac{g}{g_c} \int_{A-A_b} \left(y_2 - y_1\right) 2\pi r \, dr \qquad \text{(A5)}$$

However,

$$\int_{A-A_B} \left(y_2 - y_1\right) 2\pi r \, dr$$

is the total volume of the bubble minus the volume directly over the base. Therefore,

$$F_B = \rho_\ell \frac{g}{g_c} \left(V - V_b\right)$$

APPENDIX B

PRESSURE FORCE CALCULATIONS

The net upward pressure force acting on a differential bubble surface area directly over the base (fig. 22, p. 35) is

$$dF_P = \left(P_i - P_o\right) \cos \alpha \, dA \tag{B1}$$

Assuming that the top of the bubble is a segment of a sphere with radius of curvature T,

$$\left(P_i - P_o\right) = \frac{2\sigma_{sat}}{T} \tag{B2}$$

(ref. 28) and

$$\cos \alpha \, dA = 2\pi r \, dr \tag{B3}$$

Substituting (B2) and (B3) in (B1) yields

$$\int dF_P = \frac{2\sigma_{sat}}{T} \int_0^{R_b} 2\pi r \, dr \tag{B4}$$

Integrating gives

$$F_P = \frac{2\pi\sigma_{sat} R_b^2}{T} \tag{B5}$$

which can be expressed in terms of the base diameter as

$$F_P = \frac{1}{2}\left(\frac{\pi D_b^2}{T}\right)\sigma_{sat} \tag{B6}$$

REFERENCES

1. Siegel, R.; and Usiskin, C.: A Photographic Study of Boiling in the Absence of Gravity. J. Heat Trans., vol. 81, no. 3, Aug. 1959, pp. 230-236.

2. Usiskin, C. M.; and Siegel, R.: An Experimental Study of Boiling in Reduced and Zero Gravity Fields. J. Heat Trans., vol. 83, no. 3, Aug. 1961, pp. 243-253.

3. Siegel, R.; and Keshock, E. G.: Effects of Reduced Gravity on Nucleate Boiling Bubble Dynamics in Saturated Water. A.I.Ch.E. J., vol. 10, no. 4, July 1964, pp. 509-517.

4. Keshock, Edward G.; and Siegel, Robert: Forces Acting on Bubbles in Nucleate Boiling Under Normal and Reduced Gravity Conditions. NASA TN D-2299, 1964.

5. Sherley, J. E.: Nucleate Boiling Heat-Transfer Data For Liquid Hydrogen at Standard and Near Zero Gravity. Advances in Cryogenic Eng., K. D. Timmerhaus, ed., Plenum Press, 1963, vol. 8, pp. 495-500.

6. Zara, Eugene A.: Boiling Heat Transfer in Zero Gravity. RTD Tech. Briefs, Headquarters Res. and Tech. Div., Bolling AFB, vol. 2, no. 1, Jan. 1964, pp. 8-15.

7. Clodfelter, Robert G.: Low-Gravity Pool-Boiling Heat Transfer. Rep. No. APL-TDR-64-19 (DDC AD-437803), Air Force Systems Command, Aero Prop. Lab., Mar. 1964.

8. Merte, H., Jr.; and Clark, J. A.: Boiling Heat Transfer With Cryogenic Fluids at Standard, Fractional, and Near-Zero Gravity. J. Heat Transfer, vol. 86, no. 3, Aug. 1964, pp. 351-359.

9. Siegel, Robert; and Keshock, Edward G.: Nucleate and Film Boiling in Reduced Gravity From Horizontal and Vertical Wires. NASA TR R-216, 1965.

10. Hsu, Yih-Yun; and Graham, Robert W.: An Analytical and Experimental Study of the Thermal Boundary Layer and Ebullition Cycle in Nucleate Boiling. NASA TN D-594, 1961.

11. Chun, Ke-Sang: A Study of Steam Bubbles in Nucleate Boiling. Ph.D. Thesis, Illinois Inst. Tech., 1956.

12. Han, Chi-Yeh; and Griffith, Peter: The Mechanism of Heat Transfer in Nucleate Pool Boiling. I - Bubble Initiation, Growth and Departure. Int. J. Heat Mass Transfer, vol. 8, no. 6, June 1965, pp. 887-904; II - The Heat Flux - Temperature Difference Relation. op. cit., pp. 905-914.

13. Gaertner, R. F.: Photographic Study of Nucleate Pool Boiling on a Horizontal Surface. J. Heat Trans., vol. 87, no. 1, Feb. 1965, pp. 17-29.

14. Ellion, Max E.: A Study of the Mechanism of Boiling Heat Transfer. Memo. 20-88, California Inst. Tech., Jet Prop. Lab., Mar. 1954.

15. Merte, Herman, Jr.; and Clark, J. A.: Pool Boiling in An Accelerating System. J. Heat Trans., vol. 83, no. 3, August 1961, pp. 233-242.

16. Costello, Charles P.; and Tuthill, William E.: Effects of Acceleration of Nucleate Pool Boiling. Chem. Eng. Progr. Symposium Ser., vol. 57, no. 32, 1961, pp. 189-196.

17. Graham, Robert W.; Hendricks, Robert C.; and Ehlers, Robert C.: Analytical and Experimental Study of Pool Heating of Liquid Hydrogen Over a Range of Accelerations. NASA TN D-1883, 1965.

18. Warner, Gary E.: An Experimental Study of Subcooled Nucleate Pool Boiling. M.S. Thesis, Univ. of Denver, 1964.

19. Rehm, Thomas R.: Gravity As a Removal Force in Nucleate Boiling. Paper Presented at the Symposium on the Effects of Zero Gravity on Heat Transfer and Fluid Flow, 55th National Meeting, A.I.Ch.E., Houston, Texas, Feb. 1965.

20. Rehm, Thomas R.: Subcooled Boiling in a Negligible Gravity Field. Rep. No. DRI-2227, Univ. of Denver, May 17, 1965.

21. Adelberg, M.: Effect of Gravity Upon Nucleate Boiling. Physical and Biological Phenomena in a Weightless State. Vol. 14 of Advances in the Astronautical Sciences, Elliot T. Benedikt and Robert W. Halliburton, eds., Western Periodicals, 1963, pp. 196-222.

22. Forster, H. K.; and Zuber, N.: Growth of a Vapor Bubble in a Superheated Liquid. J. Appl. Phys., vol. 25, no. 4, Apr. 1954, pp. 474-478.

23. Zuber, Novak: Recent Trends in Boiling Heat Transfer Research. Part I: Nucleate Pool Boiling. Appl. Mech. Rev., vol. 17, no. 9, Sept. 1964, pp. 663-672.

24. Zuber, Novak: Nucleate Boiling. The Region of Isolated Bubbles and the Similarity With Natural Convection. Int. J. Heat Mass Trans., vol. 6, Jan. 1963, pp. 53-78.

25. Zemansky, Mark W.: Heat And Thermodynamics. McGraw-Hill Book Co. Inc., 1957, p. 291.

26. Fritz, W.: Maximum Volume of Vapour Bubbles. Phys. Zeits., vol. 36, June 1, 1935, pp. 379-384.

27. Staniszewski, Bogumil E.: Nucleate Boiling Bubble Growth and Departure. Tech. Rep. No. 16, Massachusetts Inst. Tech., Aug. 1959.

28. Reynolds, William C.: Hydrodynamic Considerations For The Design of Systems for Very Low Gravity Environments. Tech. Rep. No. LG-1, Stanford University, Sept. 1, 1961.

A motion-picture film supplement C-246 is available on loan. Requests will be filled in the order received. You will be notified of the approximate date scheduled.

The film (16 mm, 11 minutes, color, sound) shows the effect of subcooling and gravity level on the characteristics of water vapor generated on a flat horizontal surface.

Film supplement C-246 is available on request to

Chief, Technical Information Division (5-5)
National Aeronautics and Space Administration
Lewis Research Center
21000 Brookpark Road
Cleveland, Ohio, 44135

CUT

Date _____

Please send, on loan, copy of film supplement C-246 to
TN D-

_____

Name of organization

_____

Street number

_____

City and State Zip code

Attention: Mr. _____

Title _____

"The aeronautical and space activities of the United States shall be conducted so as to contribute . . . to the expansion of human knowledge of phenomena in the atmosphere and space. The Administration shall provide for the widest practicable and appropriate dissemination of information concerning its activities and the results thereof."

—NATIONAL AERONAUTICS AND SPACE ACT OF 1958

NASA SCIENTIFIC AND TECHNICAL PUBLICATIONS

TECHNICAL REPORTS: Scientific and technical information considered important, complete, and a lasting contribution to existing knowledge.

TECHNICAL NOTES: Information less broad in scope but nevertheless of importance as a contribution to existing knowledge.

TECHNICAL MEMORANDUMS: Information receiving limited distribution because of preliminary data, security classification, or other reasons.

CONTRACTOR REPORTS: Technical information generated in connection with a NASA contract or grant and released under NASA auspices.

TECHNICAL TRANSLATIONS: Information published in a foreign language considered to merit NASA distribution in English.

TECHNICAL REPRINTS: Information derived from NASA activities and initially published in the form of journal articles.

SPECIAL PUBLICATIONS: Information derived from or of value to NASA activities but not necessarily reporting the results of individual NASA-programmed scientific efforts. Publications include conference proceedings, monographs, data compilations, handbooks, sourcebooks, and special bibliographies.

Details on the availability of these publications may be obtained from:

SCIENTIFIC AND TECHNICAL INFORMATION DIVISION

NATIONAL AERONAUTICS AND SPACE ADMINISTRATION

Washington, D.C. 20546